Journal of Electroanalytical Chemistry 783 (2016) 106–111

Contents lists available at ScienceDirect

Journal of Electroanalytical Chemistry

journal homepage: www.elsevier.com/locate/jelechem

Effects of the electrochemically grown hydrous oxide on the hydrogen electrode reaction on iridium electrode

María A. Montero, María R. Gennero de Chialvo, Abel C. Chialvo *

Instituto de Química Aplicada del Litoral, IQAL (UNL-CONICET), Programa de Electroquímica Aplicada e Ingeniería Electroquímica, PRELINE (FIQ-UNL), Santiago del Estero 2829, Santa Fe, Argentina

ARTICLE INFO

Article history:
Received 3 September 2016
Received in revised form 8 November 2016
Accepted 14 November 2016
Available online 16 November 2016

Keywords:
Hydrogen reaction
Iridium electrode
Hydrous oxide

ABSTRACT

The hydrogen electrode reaction was studied on iridium electrodes covered by a hydrous oxide film in acid solution. The $IrO_x.nH_2O$ film was prepared by the application of repetitive cyclic voltammetry and it was characterized by the charge of the broad voltammetric peak at 0.97 V. It was observed for charges lower than 720 μC cm^{-2} a slight increase of both, the H_{UPD} electroadsorption and the steady state limiting current of hydrogen oxidation, with respect to Ir metal. For higher oxide charge values, both variables decrease while a small anodic peak appears at 0.65 V. This behaviour was explained on the basis of the formation of two types of Ir oxide depending on the film thickness and the water concentration profile, which changes the site where the hydrogen reaction takes place.

1. Introduction

The iridium electrode, unlike the rest of the noble metals, has a great ability to form thick films of hydrous oxides [1–8]. It is known that when it is subjected to a repetitively linear cyclic voltammetry perturbation in 0.5–1 M H_2SO_4 solution between a lower potential E_l near zero (vs. RHE) and an upper potential $E_u \geq 1.40$ V at sweep rates comprised in the range 0.04–0.15 V s^{-1} [1–6], a thick layer of hydrous oxide ($IrO_x.nH_2O$) is formed. This film is also obtained by the application of a square wave potential signal, between the same potential limits or with lower values of E_u [7,8]. The oxide layer is visualized in a potentiodynamic profile as a reversible couple in the potential region comprised between 0.7 V and 1.2 V, with a current peak at 0.96 V. Moreover, the film obtained exhibits a markedly different behaviour with respect to the other noble metals. The most important characteristics are: (i) oxide layer grows with the increase of the number of applied potentiodynamic cycles (triangular sweep or square wave), it is amorphous, its stoichiometry is undefined and it is inhomogeneous in depth. It can reach a thickness equivalent to hundreds of adsorbed oxygen monolayers, as it can be derived from the charge involved in the oxidation/reduction process [6]. (ii) Oxide exhibits highly reversible redox behaviour, being the cathodic peak almost a mirror image of the anodic peak [1–8]. This redox couple corresponds to the transition Ir^{+3}/Ir^{+4} of oxide species [9–12], while it is not observed any reduction process to Ir metal yet under hydrogen evolution [13]. Moreover, a small peak can be observed at approximately 0.65 V [1–7]. (iii) Hydrous Ir oxide exhibits electrochromism, originated in the proton flow to or from the oxide layer during the oxidation/reduction process [10,11,14]. (iv) The process of adsorption/desorption of underpotentially deposited hydrogen (H_{UPD}) still takes place although the electrode surface is completely covered by the iridium hydrous oxide. It only disappears when the oxide film reaches significantly high thickness values [15]. On the other hand, it is well known that the inhibition of the H_{UPD} adsorption sites is always accompanied by a decrease in the reaction rate of the hydrogen evolution [16,17], although the surface sites involved are different. All these aspects emphasize the role played by the Ir electrode pretreatment on its electrocatalytic activity towards hydrogen electrode reaction (HER). It has been already studied on iridium electrodes on both overpotential regions, that corresponding to the hydrogen evolution reaction and that where the hydrogen oxidation reaction takes place [18,19]. The electrode was previously subjected to a thermal treatment under hydrogen atmosphere in order to ensure that the reaction took place on metallic iridium. On the other hand, G. Bronöel and M. Haim [20] studied the hydrogen oxidation on an Ir electrode previously subjected to 200 voltammetric cycles between 0.03 ≤ E / V (vs. RHE) ≤ 1.40 in sulphuric acid solution. Although the authors did not include a voltammogram of the cycled electrode, it should be covered by the hydrous oxide film and therefore the results obtained cannot be compared with those recorded on Ir metal.

Taking into account that the voltammetric cycling technique, widely used as electrode pretreatment, produces on iridium the formation of an

* Corresponding author.
E-mail address: achialvo@fiq.unl.edu.ar (A.C. Chialvo).

http://dx.doi.org/10.1016/j.jelechem.2016.11.037
1572-6657/

irreducible oxide layer, the objective of the present work is the analysis of the influence of the oxide growth process on the hydrogen electrode reaction in acid solution.

2. Materials and methods

2.1. Electrode preparation

The iridium electrodes were prepared via sputtering on a glassy carbon (GC) substrate from an iridium target (Goodfellow) in an argon atmosphere (0.1 mbar), using a sputter coater Emitech K500X, operated at 30 mA during 4 min. The glassy carbon (SPI) substrate was previously mirror polished and subjected to ultrasonic cleaning in ultra-pure water for 5 min and then was voltammetrically characterized to ensure a clean and reproducible deposition surface. In order to have an initial surface free of oxide, the iridium electrodes were annealed in a tubular furnace at 600 °C during 30 min in hydrogen atmosphere and then cooled in the same environment.

The development of the oxide layer was carried out following the procedure proposed by J.O. Zerbino et al. [3]. It consisted in the application of repetitive cyclic voltammetry between $-0.07 < E\ (\text{vs. RHE})\ / \text{V} < 1.66$ at a sweep rate of 0.15 V s^{-1}. The thickness of the resulting oxide layer was modified varying the time of cycling.

2.2. Electrochemical measurements

All the electrochemical experiments were carried out in a three electrode cell. The electrolyte solution was 0.5 M H_2SO_4. The reference electrode was a hydrogen bubble electrode in the same solution (RHE), located inside a Luggin-Haber capillary tube. The counter electrode was a platinum wire of high area, located in a separate compartment in order to avoid contamination. Ultra pure water (resistivity 18.2 MΩ) was employed for cell rinsing and solution preparation. The working electrode was mounted in a Teflon holder, with a geometric exposed area of 0.167cm^2 and connected to a rotating disc device. The rotation rate was varied between $900 \le \omega \le 3600$. The electrodes were electrochemically characterized via cyclic voltammetry between 0.0 and 1.3 V at 0.1 V s^{-1} under nitrogen atmosphere after the thermal treatment under H_2 as well as after the growth of the oxide layer. All experiments were carried out at room temperature (295 K).

2.3. Electrode characterization

The surface morphology of the electrodes was characterized by Atomic Force Microscopy (AFM), using an Agilent 5400 microscope operated in tapping mode and the images were processed with the software WSxM 6.2. EDS spectra were also obtained with a Microscope Phenom World ProX operated at 15 kV for superficial composition determination.

The amount of adsorption sites accessible to the reaction intermediate species on the Ir metal surface when it is covered by a hydrous oxide layer was evaluated through the charge of H_{UPD} obtained by cyclic voltammetry.

2.4. Evaluation of the current-overpotential dependence

The current (I) - overpotential (η) curves of the hydrogen electrode reaction on the hydrous iridium oxide electrode were evaluated under continuous hydrogen bubbling to ensure the solution saturation, through the application of a potential program and the acquisition of the current response at different rotation rates. These measurements were carried out using a potentiostat Wenking POS2, connected to a PC via an Advantech PCI1710HG interface and operated with the software Labview®. Once the working electrode reached the equilibrium potential (0.0 ± 0.002 V vs. RHE), the potential program was applied, which consisted in 3 s at 0.0 V, followed by 5 s at the desired overpotential value. In this last period, readings of the current value were made each 0.01 s and the mean value of the current data measured in the last second was assigned to the step overpotential. Then the program was repeated for each η value, which was varied in the range $-0.015 \le \eta / \text{V} \le 0.30$. Four rotation rates were employed, varied between $900 \le \omega / \text{rpm} \le 3600$.

3. Results

3.1. Electrode characterization

Fig. 1 shows the voltammograms corresponding to the Ir electrode before (a) and after (b) the application of the procedure for the formation of the hydrous oxide layer. The voltammetric profile shown in curve (a) corresponds to that expected for metallic iridium [1,13,21], where it can be observed the peaks corresponding to electroadsorption/desorption of H_{UPD}. Moreover, the voltammogram of the same electrode covered by a thick oxide layer is depicted in curve (b). It can be appreciated the presence of a wide anodic peak centred at 0.96 V and at almost the same potential value the corresponding cathodic reduction peak. It can be also observed a small anodic peak located at 0.65 V, but the corresponding cathodic peak is not found. When the anodic limit of the potentiodynamic sweep is set immediately after this peak (0.70 V) it can be appreciated a quasi reversible response, which cannot be perceived in the extended voltammogram. As it has been already mentioned, this voltammetric profile is typical of the Ir electrode covered by a thick layer of hydrous oxide [1–7,15]. Moreover, it can be noticed the disappearance of the peaks corresponding to the adsorption/desorption of H_{UPD}. The variation of the charge of these peaks with the thickness of the oxide layer will be analysed later.

Fig. 2 shows the AFM image obtained for iridium electrode before (a) and after (b) the formation of the hydrous oxide layer. It can be observed in micrograph (a) that Ir electrode is constituted by nanoparticles of approximately 50 nm diameter. The EDS analysis shows only the presence of carbon (substrate) and iridium. The surface covered by the oxide layer (micrograph (b)) shows a smoother morphology with loss of definition of the nanoparticles due to the development of the oxide film. The corresponding EDS profile shows peaks of C, Ir and O.

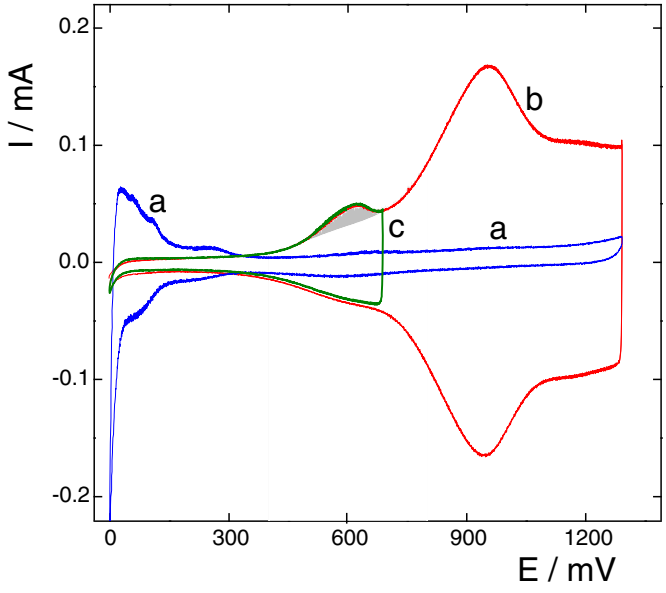

Fig. 1. Voltammetric profile of the Ir electrode run at 0.1 V s^{-1} in 0.5 M H_2SO_4. (a) Ir metal; (b) Ir oxide electrode; (c) upper potential limit 0.7 V.

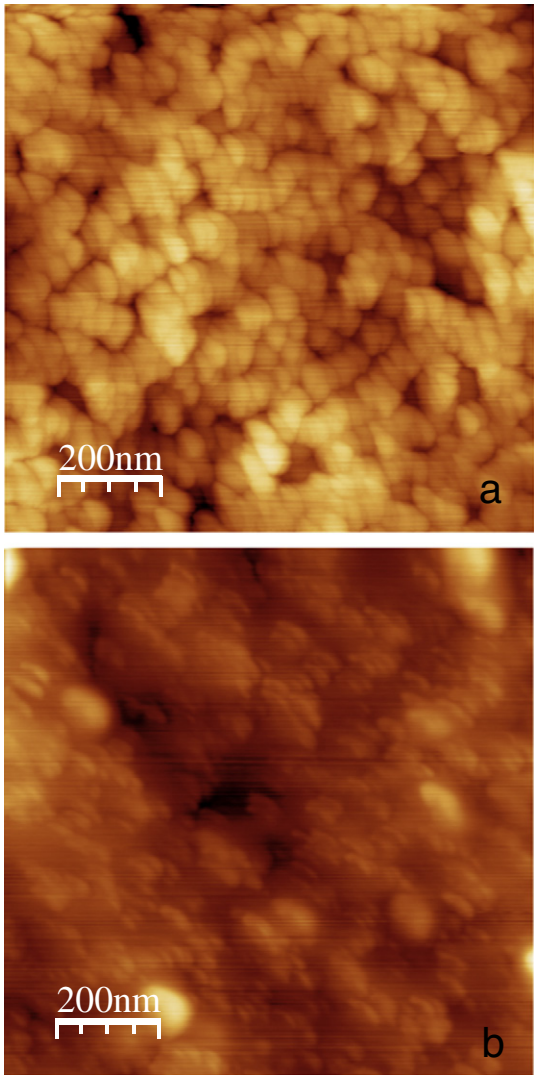

Fig. 2. AFM images of the Ir electrode. (a) before and (b) after the oxidation treatment.

3.2. Relationship between anodic oxide peaks

Fig. 3 illustrates the voltammograms obtained for the Ir electrode with increasing oxide charge. Starting from them, the variation of the anodic charge of the main peak as a function of the respective charge of the small peak at 0.65 V can be evaluated (shaded area in Fig. 1). This relationship is depicted in Fig. 4, where it can be appreciated that the charge of the main peak located at 0.96 V must reach a critical value near 720 μC cm^{-2} (referred to the geometric area) before the small peak can be noticed. Once reached this condition, both peaks charges increases.

3.3. Effects of the thickness film on H_{UPD} process

The analysis of the voltammograms of Fig. 3 indicates that in the initial stages (low oxide charges) it can be only observed the main peak at 0.96 V, as well as those corresponding to the process of adsorption/desorption of H_{UPD}. However, as the charge of the hydrous oxide increases, the appearance of a small peak at 0.65 V slows down the increase in the H_{UPD} charge. In order to quantify this effect, the electrodesorption charge of H_{UPD} was depicted as a function of the charge of the small peak, which is shown in Fig. 5. It can be clearly observed that the H_{UPD} charge reaches a maximum value, then decreases and finally turns to

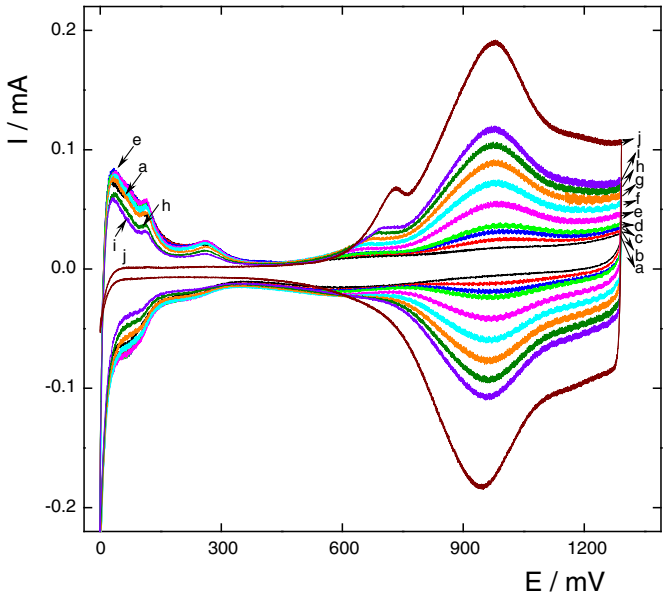

Fig. 3. Voltammetric profile of the Ir electrode with different oxide charges (μC cm^{-2}): (a) 0; (b) 261; (c) 472; (d) 530; (e) 720; (f) 1347; (g) 1950; (h) 2556; (i) 3605; (j) 6890. 0.1 V s^{-1}; 0.5 M H_2SO_4.

be negligible. This result is particularly important, as it allows relating the inhibition of the H_{UPD} adsorption with the oxidation process involved in this peak.

3.4. Hydrogen electrode reaction

The hydrogen electrode reaction was experimentally studied on the hydrous iridium oxide electrodes. The study was carried out in the overpotential range $-0.015 \le \eta / V \le 0.30$ at rotation rates varying between $900 \le \omega / rpm \le 3600$. After the voltammetric characterization, the solution was saturated with hydrogen. Once the equilibrium potential (0.0 ± 0.002 V vs. RHE) was reached, it was applied the potential program described previously and the current response was acquired. The kinetic response was analysed on electrodes prepared with

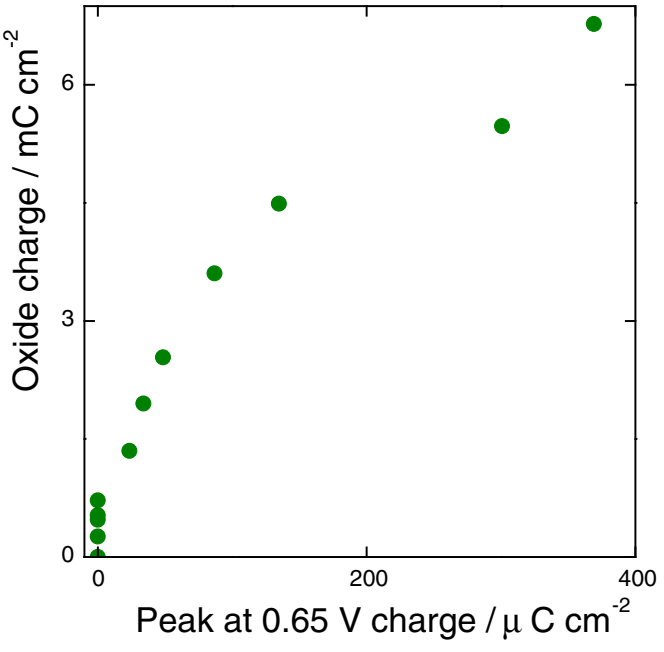

Fig. 4. Relationship between the oxide charge and the peak at 0.65 V charge.

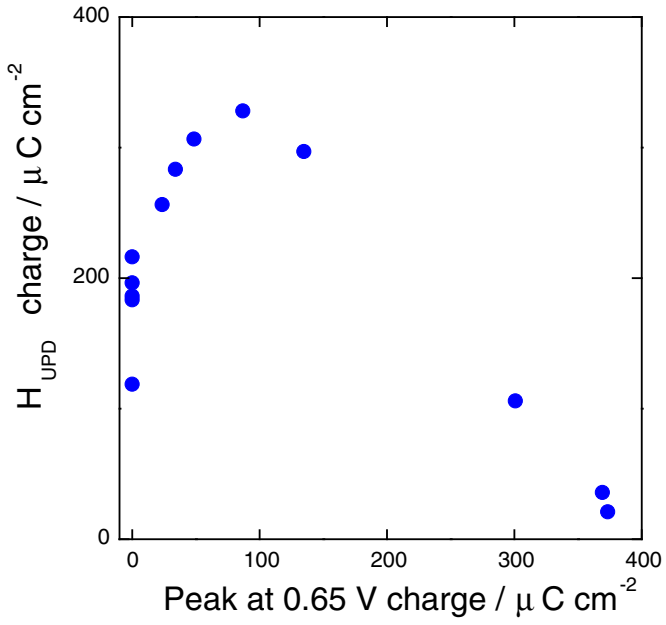

Fig. 5. Relationship between the H_{UPD} charge and the peak at 0.65 V charge.

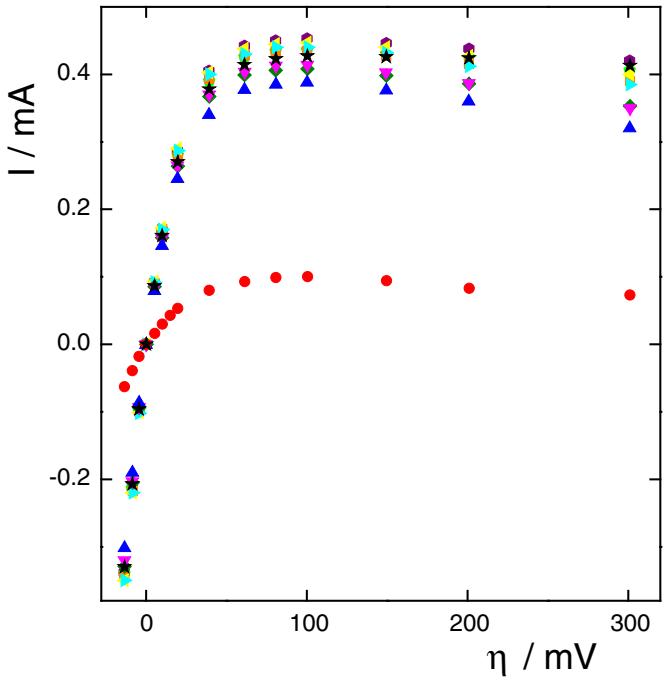

Fig. 7. Current vs. overpotential plot of the HER on the Ir electrode with different oxide charges (μC cm^{-2}): (★) 0; (●) 261; (⬟) 472; (■) 530; (◄) 720; (►) 1347; (◆) 1950; (▼) 2556; (▲) 3605; (●) 6890. $\omega = 2500$ rpm; 0.5 M H_2SO_4.

different oxide layer thicknesses. Fig. 6 shows the current-time plot resulting from the potential program applied to an electrode with a hydrous oxide charge equal to 530 μC cm^{-2}. It can be appreciated that the response is qualitatively similar to that observed on metallic Ir in the same solution [18]. It should be noticed particularly that the system quickly reaches the equilibrium potential after each polarization value, either anodic or cathodic. Moreover, the effect of the thickness of the oxide layer on the current-overpotential dependence on steady state is illustrated in Fig. 7, at a rotation rate of 2500 rpm. It can be appreciated that at low thicknesses, when the charge of the hydrous oxide is < 720 μC cm^{-2}, current increases slightly with respect to the value corresponding to Ir metal (symbol ★). Nevertheless when this value is overcame, which corresponds to the appearance of the small peak at 0.65 V

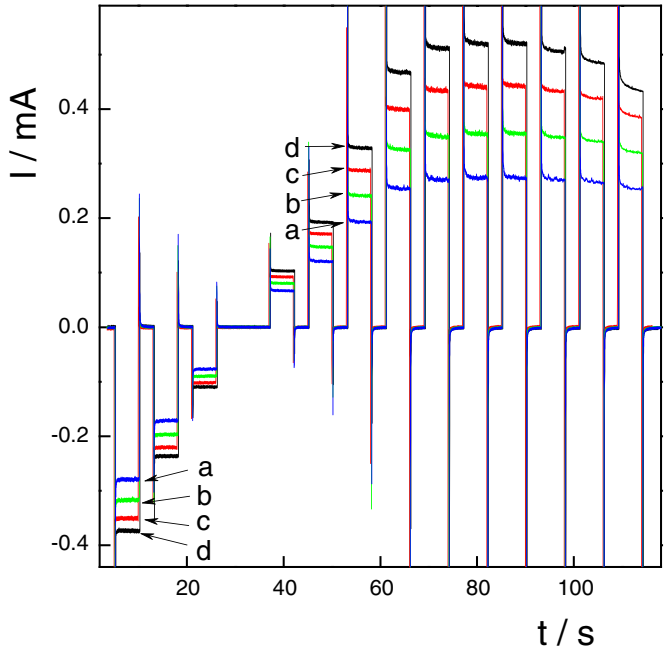

Fig. 6. Current vs. time response of Ir electrode with oxide charge 530 μC cm^{-2} to the program applied in the range − 0.015 V ≤ η ≤ 0.30 V for HER evaluation. ω (rpm): (a) 900; (b) 1600; (c) 2500; (d) 3600.

in the voltammetric profile, a significant decrease of the current values is observed. For the oxide layer thickness where the charge of H_{UPD} is negligible (6890 μC cm^{-2}), a decrease in the order of 75% with respect to metallic Ir was found (Fig. 7, curve j).

4. Discussion

4.1. Interpretation of hydrous Ir oxide voltammetric behaviour

The results obtained show that thin hydrous oxide layers voltammetrically grown on Ir do not affect significantly the experimental current-overpotential dependence of the hydrogen electrode reaction (Fig. 7). The same influence was found on the adsorption of the underpotentially deposited hydrogen H_{UPD} (Fig. 5). Nevertheless, once a critical thickness is overcome, both processes are unfavourably influenced. Consequently, taking into account that the inhibition of the adsorption sites of the H_{UPD} affects the behaviour of the reaction intermediate of the hydrogen electrode reaction and therefore the reaction rate [16,17], the identification of the source of such inhibition will facilitate the understanding of the kinetics of the reaction on this type of electrodes. The analysis of the results obtained for both, the HER and the H_{UPD} adsorption, allowed to establish two distinctive behaviours as a function of the thickness of the oxide layer (quantified by the voltammetric charge related to the geometric area). For oxide charges up to 720 μC cm^{-2}, the electroadsorption charge of H_{UPD} increases slightly with oxide charge. As H_{UPD} charge is proportional to the free iridium surface, it can be concluded that: (i) there is an increase in the Ir surface roughness due to its dissolution, needed for the formation of the oxide layer, and (ii) the hydrous oxide layer has a behaviour similar to that of the electrolytic solution and thus the HER can take place on the Ir surface. For these charge values (<720 μC cm^{-2}), the voltammetric profile shows only one broad peak of electrooxidation located at 0.96 V. As the cycling time is increased, the hydrous oxide charge increases and a small anodic peak appears in the ascending branch of the main peak, located near 0.65 V. As it can be observed in Fig. 5, this process is accompanied first by an increase and then by a gradual decrease of the electroadsorption H_{UPD} charge. This behaviour

is explained on the basis of a competition between the increase in the Ir surface roughness due to its dissolution and the H_{UPD} inhibition process. Consequently, as the appearance of this peak coincides with the initiation of the inhibition of the H_{UPD} adsorption, this behaviour can be attributed to the formation of a different type of oxide with respect to that involved in the main voltammetric peak. Explanations about the origin of this peak in the literature are scarce. It was assigned by L.D. Burke and D.P. Whelan [22] to the transition Ir^{+3}/Ir^{+4} in species containing sulphate inside the coordination sphere. Then, it was studied with more detail by I.T.E. Fonseca et al. [15], who concluded that it is due to the formation of IrOOH or else a film of polymeric nature. However, these processes cannot explain the H_{UPD} inhibition. Moreover, there is a fairly widespread agreement [6,23–25] in that this type of oxide films consists in two layers. The inner layer is compact, anhydrous or scarcely hydrated, with a thickness of a few monolayers. Then there is an outer layer in contact with the electrolyte solution, which is highly hydrated and significantly thicker. The mechanism by which the H_{UPD} inhibition process takes place can be understood on the basis of a reinterpretation of the model of the double oxide layer considering the dynamic character of its growth process. During the anodic sweep, Ir surface releases electrons and reacts with the superficial water network to produce a hydrous Ir(III) oxide, which is then oxidized to an also hydrated Ir(IV) oxide, process that is accompanied by the release of H^+. This initial oxide layer is incorporated to the water network that surrounds the electrode surface. During the cathodic sweep, Ir(IV) oxide is reduced to the Ir(III) compound inside the water network. The subsequent cycles incorporate new superficial Ir atoms to the oxide film and also oxidize the pre-existent reduced form. The final result of the whole process is a polymeric cross-linked film constituted by Ir oxide species and water in a complex structure with a gel consistency. The electric conduction in the film is basically protonic, through a Grotthus type mechanism. As the oxide film grows, the water diffusion through this gel-like structure turns to be more difficult and thus its concentration near the metallic surface decreases. On these conditions, the hydrous oxide adjacent to the surface actuates as a water source and begins to be dehydrated and spatially reordered, tending to an equilibrium configuration. This process ultimately leads to a highly dehydrated inner layer, with a stoichiometry similar to IrO_2 [23,25], showing electronic conduction properties [26,27]. The coverage of the iridium surface with this almost anhydrous oxide is the responsible of the inhibition of the H_{UPD} adsorption, which is initiated when the oxide charge overcome the value 720 μC cm^{-2} and is completed for charges >6800 μC cm^{-2}, as it can be observed in the curve j of Fig. 3. Furthermore, Fig. 1 shows also that, although the H_{UPD} sites are totally inhibited, a cathodic current corresponding to hydrogen evolution can be still observed. This result indicates that this reaction is verified although the sites on Ir metal are not available. A similar behaviour exhibits the IrO_2 electrode, where the hydrogen evolution can be appreciated in absence of the peaks corresponding to the H_{UPD} adsorption [28,29]. In this context, the process verified at the voltammetric peak at 0.65 V can be assigned to the pseudocapacitive response originated in the electroadsorption of water in the interphase between the inner oxide layer and the hydrous gel-type oxide layer. This process is quasi reversible, as it is illustrated in the curve c of Fig. 1. The absence of the corresponding cathodic peak in the extended voltammogram (Fig. 1, curve a) is due to that the cathodic processes involve basically the same species for both peaks. Therefore, it can be concluded that the determining factor of the electrochemical behaviour of the oxide film is the profile of the water concentration along the film thickness, resulting from the anodic and cathodic processes during the oxide growth. As a result, an inner layer almost anhydrous and an outer layer of gel-type oxide are formed. Fig. 8 illustrates qualitatively the local concentration profile of water for different thicknesses of the $IrO_x \cdot nH_2O$ film. Consequently, during the voltammetric sweeps there is an oxidation of the superficial Ir atoms and a net diffusion of water towards the metal surface, together with an in/out flow of protons that neutralizes the electrons involved in the Ir oxidation. Thus,

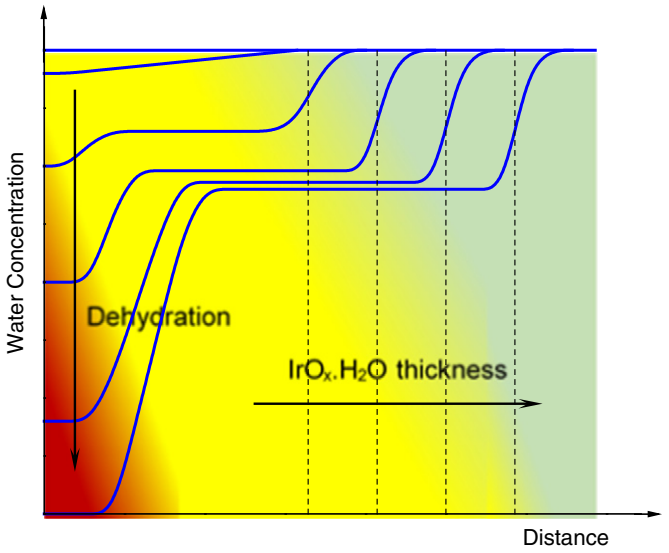

Fig. 8. Scheme of water concentration profile inside the oxide film for different film thicknesses.

the origin of the inner layer is a consequence of the dehydration of the metal/solution interface do to the formation of oxide from Ir and water.

4.2. Interpretation of the hydrogen oxidation inhibition

The analysis carried out in the previous item shows that the place on which the hydrogen evolution/oxidation is developed depends strongly on the thickness of the hydrous oxide film. For charges lower than 720 μC cm^{-2}, the absence of the inner anhydrous layer allows the diffusion of molecular hydrogen through the whole oxide film, so that it can react on metal Ir sites. Thus, for these low oxide charge values the hydrous gel-type oxide layer behaves like the aqueous electrolyte solution. On the other hand, when the growth of the inner layer inhibits the H_{UPD} adsorption (oxide charge > 6800 μC cm^{-2}), which implies the absence of free sites on the Ir surface, the hydrogen oxidation/reduction must be verified on the interphase between the inner and the hydrous oxide layers. Moreover, the decrease in the limiting diffusion current (Fig. 7, line j) is due to that this current is limited by the hydrogen diffusion through the hydrous oxide layer [30,31]. The behaviour of the inner oxide layer is similar to that observed on IrO_2 electrodes, as it is well known that this oxide catalyzes the hydrogen evolution [32,33]. Finally, there is a range of oxide layer charges, between 720 and 6800 μC cm^{-2}, where the hydrogen electrode reaction takes place on two different surfaces. One of them is the Ir metal sites, where the HER is verified through the Volmer-Heyrovsky-Tafel mechanism [18,19]. The other is the surface of the anhydrous inner oxide, where the reaction takes place through different reaction intermediates and/or a different kinetic mechanism [32,33].

5. Conclusions

On the basis of the evaluation of the charges involved in the voltammetric peaks corresponding to H_{UPD} electroadsorption, to the couple Ir^{+3}/Ir^{+4} of the hydrous Ir oxide and that of the small anodic peak at 0.65 V, the behaviour of the hydrogen electrode reaction on this type of electrodes could be explained. It was demonstrated that the growth of the oxide film is determined by the requirement of water as a source of oxygen. Depending on the film thickness, two types of Ir oxides are developed. The inner oxide, almost anhydrous, is an electronic conductor similar to IrO_2. The outer oxide layer is highly hydrated with a gel-like structure. It was found that, for the preparation conditions used, there is a threshold charge of 720 μC cm^{-2} below

which the inner layer is not formed. On these conditions the hydrogen electrode reaction is verified on the Ir metal. On the other hand, when the oxide charge is higher than 6800 C cm^{-2}, the reaction takes place on the interphase between the inner and the hydrous oxide layers. Meanwhile, for charges ranging between those values the HER is verified simultaneously on both surfaces.

It can finally be concluded that cycling of the iridium electrodes as a pretreatment for kinetic studies deeply modifies the electrode surface through a complex process of irreducible oxides formation. Consequently, it must be ensured the absence of oxide before any study of electrocatalytic activity on iridium, by thermal treatment under H_2 atmosphere and characterization through a single potentiodynamic sweep.

Acknowledgements

The authors wish to acknowledge the financial support received from ANPCyT (PICT 1548), CONICET (PIP 0674) and UNL (CAI + D 63-91).

References

[1] D.A.J. Rand, R. Woods, J. Electroanal. Chem. 55 (1974) 375–381.
[2] D.N. Buckley, L.D. Burke, J. Chem. Soc. Faraday Trans. 71 (1975) 1447–1459.
[3] J.O. Zerbino, N.R. de Tacconi, A.J. Arvia, J. Electrochem. Soc. 125 (1978) 1266–1276.
[4] S. Gottesfeld, S. Srinivasan, J. Electroanal. Chem. 86 (1978) 89–104.
[5] E.J. Frazer, R. Woods, J. Electroanal. Chem. 102 (1979) 127–130.
[6] B.E. Conway, J. Mozota, Electrochim. Acta 28 (1983) 9–16.
[7] R. Kotz, H. Neff, S. Stucki, J. Electrochem. Soc. 131 (1984) 72–77.
[8] T. Pauporte, F. Andolfatto, R. Durand, Electrochim. Acta 45 (1999) 431–439.
[9] A. Minguzzi, O. Lugaresi, C. Locatelli, S. Rondinini, F. D'Acapito, E. Achilli, P. Ghigna, Anal. Chem. 85 (2013) 7009–7013.
[10] J.D.E. McIntyre, S. Basu, W.F. Peck Jr., W.L. Brown, W.M. Augustyniak, Phys. Rev. B 25 (1982) 7242–7254.
[11] R. Kotz, C. Barbero, O. Haas, J. Electroanal. Chem. 296 (1990) 37–49.
[12] M. Huppauff, B. Lengeler, J. Electrochem. Soc. 140 (1993) 598–602.
[13] L.D. Burke, N.S. Naser, B.M. Ahern, J. Solid State Electrochem. 11 (2007) 655–666.
[14] S. Gottesfeld, J.D.E. McIntyre, G. Beni, J.L. Shay, Appl. Phys. Lett. 33 (1978) 208–210.
[15] I.T.E. Fonseca, M.I. Lopes, M.T.C. Portela, J. Electroanal. Chem. 415 (1996) 89–96.
[16] R. Gomez, A. Fernandez-Vega, J.M. Feliu, A. Aldaz, J. Phys. Chem. 97 (1993) 4769–4776.
[17] P.M. Quaino, M.R. Gennero de Chialvo, A.C. Chialvo, J. Electrochem. Soc. 156 (2009) B167–B173.
[18] M.A. Montero, J.L. Fernández, M.R. Gennero de Chialvo, A.C. Chialvo, J. Phys. Chem. 117 (2013) 25269–25275.
[19] M.A. Montero, M.R. Gennero de Chialvo, A.C. Chialvo, J. Electroanal. Chem. 767 (2016) 153–159.
[20] G. Bronöel, M. Haim, J. Chim. Phys. 73 (1976) 952–960.
[21] I. Mozota, B.E. Conway, Electrochim. Acta 28 (1983) 1–8.
[22] L.D. Burke, D.P. Whelan, J. Electroanal. Chem. 162 (1984) 121–141.
[23] P.G. Pickup, V.I. Birss, J. Electroanal. Chem. 220 (1987) 83–100.
[24] L.D. Burke, E.J.M. O'Sullivan, J. Electroanal. Chem. 117 (1981) 155–160.
[25] J. Augustynski, M. Koudelka, J. Sanchez, B.E. Conway, J. Electroanal. Chem. 160 (1984) 233–248.
[26] S. Hackwood, A.H. Dayem, G. Beni, Phys. Rev. B 26 (1982) 471–478.
[27] J.S. Almeida, R. Ahuja, Phys. Rev. B 73 (2006) 165102–165106.
[28] T. Hepel, F.H. Pollak, W.E. O'Grady, J. Electrochem. Soc. 132 (1985) 2385–2390.
[29] S. Fierro, A. Kapalka, C. Comninellis, Electrochem. Commun. 12 (2010) 172–174.
[30] C.A. Marozzi, M.R. Gennero de Chialvo, A.C. Chialvo, Open Electrochem. J. 1 (2009) 49–55.
[31] M.S. Rau, C.A. Marozzi, M.R. Gennero de Chialvo, A.C. Chialvo, Open Electrochem. J. 2 (2010) 1–5.
[32] J.C.F. Boodts, S. Trasatti, J. Appl. Electrochem. 19 (1989) 225–262.
[33] L. Chen, D. Guay, A. Lasia, J. Electrochem. Soc. 143 (1996) 3576–3584.